

Unexpectedly wide reversible vortex region in β -pyrochlore RbOs_2O_6

Pierre Legendre, Yanina Fasano, Ivan Maggio-Aprile, Øystein Fischer
*Département de Physique de la Matière Condensée, Université de Genève,
24 Quai Ernest-Ansermet, 1211 Geneva, Switzerland*

Zbigniew Bukowski, Sergiy Katrych, Janusz Karpinski
Laboratory for Solid State Physics, ETH Zürich, 8093 Zürich, Switzerland

(Dated: December 22, 2018)

Abstract

We study the extent of the reversible region in the vortex phase diagram of recently available RbOs_2O_6 single crystals [1] by means of bulk magnetization measurements. We found that the irreversible magnetic response sets in at a field $H_{\text{irr}}(T) \sim 0.3H_{c2}(T)$ for $0.5 \lesssim T/T_c \lesssim 0.8$, yielding a reversible vortex region that is wide in comparison with other low- T_c materials. The relevance of thermal fluctuations is limited since we estimate a Ginzburg number $G_1 = 5 \times 10^{-7}$. However, the relevance of quenched disorder is low since the critical-current density ratio at low fields and temperatures is of the order of that found in high- T_c 's. We therefore conclude that an intrinsically low bulk pinning magnitude favors the existence of an unexpectedly wide reversible vortex region in RbOs_2O_6 .

INTRODUCTION

The recent discovery of superconductivity in the β -pyrochlore osmate compounds AOs_2O_6 ($A = \text{K}$ [2, 3], Rb [4, 5, 6], Cs [7]) triggered a plethora of studies on the superconducting pairing mechanism in these compounds. In spite of the active research on β -pyrochlores over the last four years, only three works report on the magnetic and spectroscopic properties of vortex matter in these compounds [8, 9, 10]. These three studies focus on KOs_2O_6 , the β -pyrochlore which presents the highest $T_c \sim 9.6 \text{ K}$ [11]. This compound has a Ginzburg-Landau parameter $\kappa = 70-87$ [12, 13] and $H_{c2}(0) = 24$ (single-crystals [12]) - 33 T (polycrystals [14]) which is larger than the Pauli paramagnetic limiting field [3]. This suggests that at very low temperatures exotic superconducting phases might be stable at high magnetic fields [3]. In the rest of the $H - T$ phase diagram conventional vortex physics is expected.

The first of these works [8] reports a low-field re-entrant behavior of the temperature at which resistance becomes negligible. The re-entrance is detected for vortices moving in particular crystallographic directions. This suggests that the phenomenon has its origin in a pinning mechanism arising from the specific crystal structure of KOs_2O_6 , indicating a resemblance to the intrinsic pinning mechanism detected in high- T_c superconductors [43].

The second of these works [9] reports a drastic change in the spatial distribution of vortices when cooling through a temperature T_p . Specific heat measurements established that KOs_2O_6 presents a first-order phase transition at an almost field-independent temperature $T_p \sim 8 \text{ K}$ [8, 12]. This transition has been associated with the freezing of the "rattling" phonon mode arising from the vibration of the K ion within the oversized Os-O cage [15]. The low temperature ($T < T_p$) vortex phase is characterized by a reduced vortex line energy [9], implying a decrease in the vortex-vortex interaction energy. This study therefore raises the question of a structural transition in the KOs_2O_6 vortex matter occurring at T_p .

The third of these works [10] reports on Scanning Tunnelling Microscopy imaging of vortices in the low temperature phase. The observed structures present significant variations in the intervortex distances. In particular, the spacing between some vortices is roughly half the average vortex lattice parameter. These findings are in agreement with a reduction of the vortex interaction energy for the phase located at $T < T_p$.

These works suggest that vortex matter in KOs_2O_6 presents unexpected properties for a low- T_c material. Therefore, studies in RbOs_2O_6 and CsOs_2O_6 are necessary to gain more

insight into the properties of vortex matter in the β -pyrochlore osmate family. This is particularly relevant since Rb and Cs β -pyrochlores do not present the first-order phase transition associated with a dramatic change in the phonon spectra in the superconducting phase [20].

In this work we study the vortex phase diagram of RbOs_2O_6 single-crystals by means of bulk magnetization measurements. Up until now, only one work reports on structural and superconducting properties of RbOs_2O_6 single crystals [1] and the rest of the literature is devoted to polycrystalline samples. The most important result reported here is that RbOs_2O_6 presents a wide reversible vortex region spanning down to a field $H_{\text{irr}}(T) \sim 0.3H_{\text{c}2}(T)$ at low temperatures. This finding is in direct contrast with results found in other low- T_c superconductors. We provide evidence that the wide reversible region originates from the small critical current density in RbOs_2O_6 . The unusually wide reversible region and the low critical current density observed in RbOs_2O_6 are consistent with the available data for KOs_2O_6 [3].

EXPERIMENTAL AND SAMPLE DETAILS

The study presented here was carried out on two RbOs_2O_6 single crystals of the same batch that provided similar results. The samples were grown in evacuated quartz ampoules following the method described in Ref. [1]. The crystals have a prism-like shape with typical dimensions $0.1 - 0.2 \times 0.2 \times 0.2 \text{ mm}^3$ and weight $49.7 - 100.2 \pm 0.1 \mu\text{g}$.

The structural properties of the crystals were investigated on a four-circle X-ray diffractometer (XCalibur PX of Oxford Diffraction with an oscillation angle of 1° and Mo $K\alpha$ radiation) equipped with a CCD area detector placed at 60 mm from the sample. The data was refined on F^2 by employing the program SHELXL-97 [16] and the results reveal a β -pyrochlore cubic structure [18, 19] (see Table I). The occupation of all elements remained 100% during the structural refinement. No additional phases (impurities, twins or intergrowth crystals) were detected by examining the reconstructed reciprocal space section shown in Fig. 1. The crystals present low mosaicity with an average mosaic spread of 0.13(3) (estimated analyzing every frame by using XCalibur with the CrysAlis Software System [17]). The observed reflections present a smaller intensity than the calculated ones (extinction coefficient $\epsilon = 64(7) \times 10^{-4}$, see Table I). This can be explained by the very small

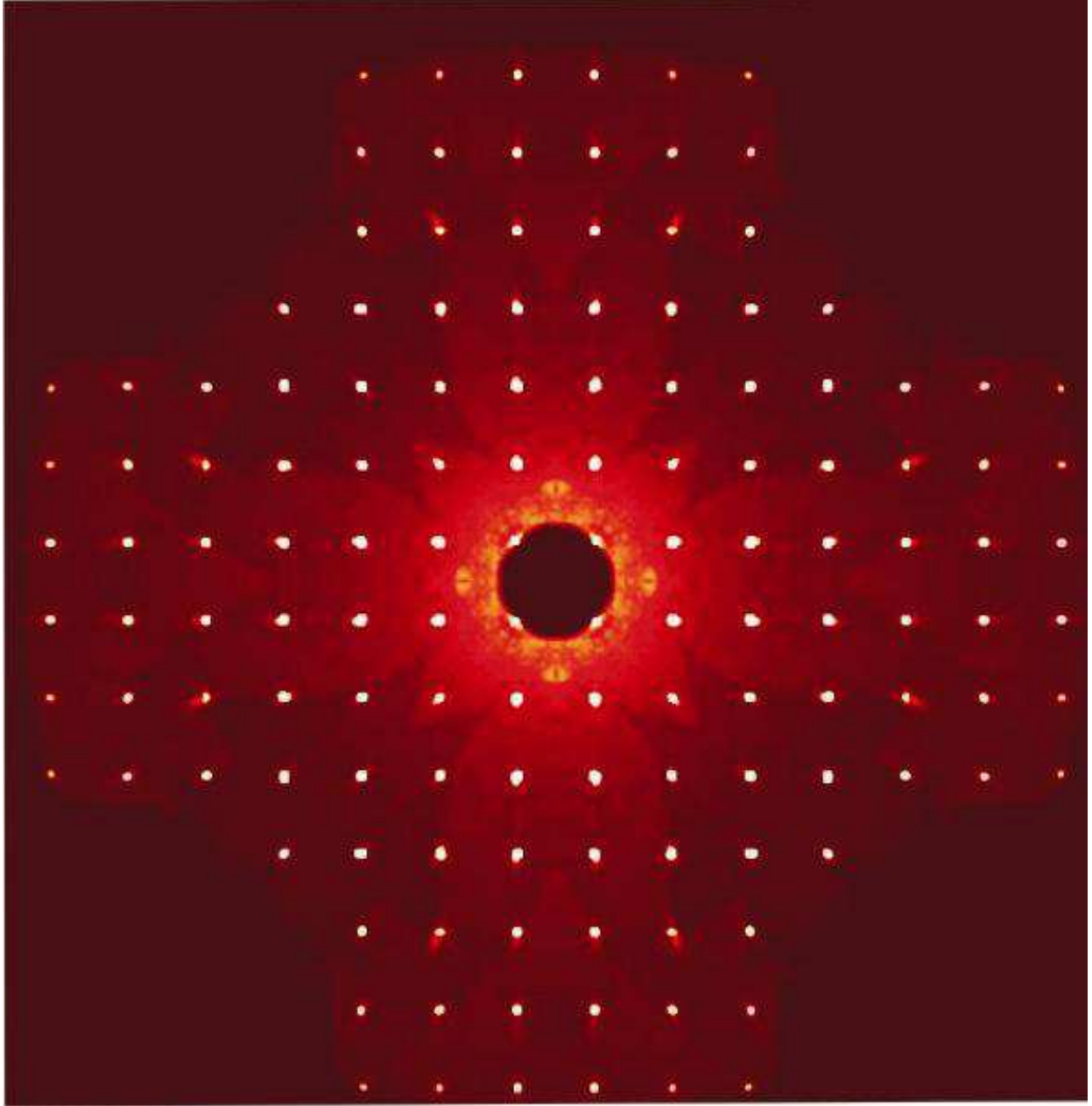


FIG. 1: Reconstructed $h1l$ reciprocal space section of a RbOs_2O_6 sample measured at 295 K.

misorientation of mosaic blocks. The reconstructed reciprocal space section and refinement results indicate that the single crystals used in this study are of a high crystalline perfection.

The superconducting magnetic properties of the samples were characterized by zero-field-cooled (ZFC) and field-cooled (FC) magnetization *vs.* temperature measurements, $M(T)$, and magnetization *vs.* magnetic field loops, $M(H)$. Measurements for applied fields

TABLE I: Structure and refinement data for RbOs_2O_6 at 295,0(5) K.

Wavelength, Å/radiation	0.71073/Mo $K\alpha$
Crystal system, space group	cubic, Fd-3m (No 227)
Unit cell dimensions, Å	a =10.1214(8)
Volume, Å ³	1036.9(4)
Z	8
Absorption correction type	analytical
Theta range for data collection, deg.	5.79 to 36.13
Limiting indices	-13≤h≤12, -14≤k≤10, -13≤l≤13
Reflections collected/unique	937/94, $R_{int} = 0.032$
Refinement method	Full-matrix least-squares on F^2
Data /restraints/parameters	94/0/7
Goodness-of-fit on F^2	1.310
Final R indices [$I > 2\sigma(I)$]	$R_1 = 0.0322$, $wR_2 = 0.0791$
R indices (all data)	$R_1 = 0.0335$, $wR_2 = 0.0808$
Extinction coefficient	0.0064(7)
$\Delta\rho_{max}, \Delta\rho_{min}$ (e/Å ³)	2.890 and -2.408

below 1.2 T were performed in a SQUID magnetometer; for larger applied fields a PPMS magnetometer was used.

RESULTS AND DISCUSSION

The critical temperature of the samples was determined by resistivity R , AC susceptibility χ' and low-field magnetization M measurements (see Fig. 2). T_c is defined as the temperature at which $\partial\chi'/\partial T$, $\partial M/\partial T$ and $\partial R/\partial T$ present a peak. The transition width is estimated as the full-width at half-maximum of these peaks. Critical temperature values of $T_c = (5.50 \pm 0.05)$ K from resistivity and (5.45 ± 0.03) K from susceptibility and magnetization were obtained. The transition width detected by susceptibility or magnetization (0.3 K) with an applied field of 11 Oe is slightly broader than the one detected by resistivity (0.2 K) at zero field. A previous work [1] reports a higher T_c value for RbOs_2O_6 single-crystals, but

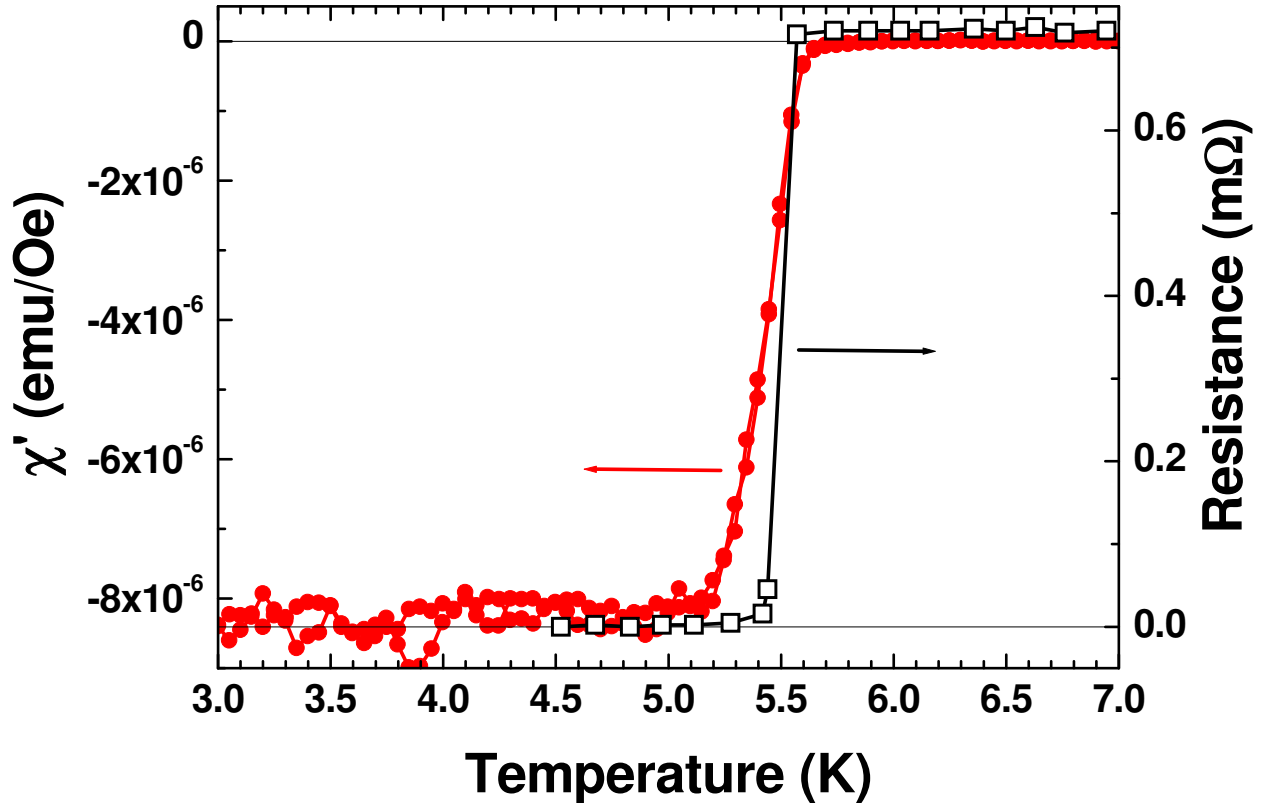


FIG. 2: (a) Superconducting transition of one of our RbOs_2O_6 crystals at zero field as detected by resistivity (open black symbols) and the real component of the AC susceptibility (full red symbols). AC Susceptibility measurements were performed with an applied field of 5 Oe at 970 Hz.

this property is known to be strongly dependent on the sample disorder or small natural variations in stoichiometry.

The superconducting fraction of the sample was obtained from the Meissner slope of the virgin branch of $M(H)$ loops such as the one shown in Fig.3b. After correcting for demagnetization effects, we estimated our samples have a superconducting fraction of 85 – 100 %. Together with the fact that the onset of the superconducting transition detected from susceptibility measurements coincides with the temperature at which resistance becomes negligible, this result indicates that the samples undergo a bulk superconducting transition.

In order to determine the $H - T$ vortex phase diagram of RbOs_2O_6 we obtained the upper critical field line $H_{c2}(T)$ and the irreversibility line $H_{\text{irr}}(T)$ from FC-ZFC $M(T)$ measurements. Typical $M(T)$ curves for an applied field of 100 Oe are shown in Fig. 4. For all applied fields the value of the ZFC magnetization at low temperatures gives a superconduct-

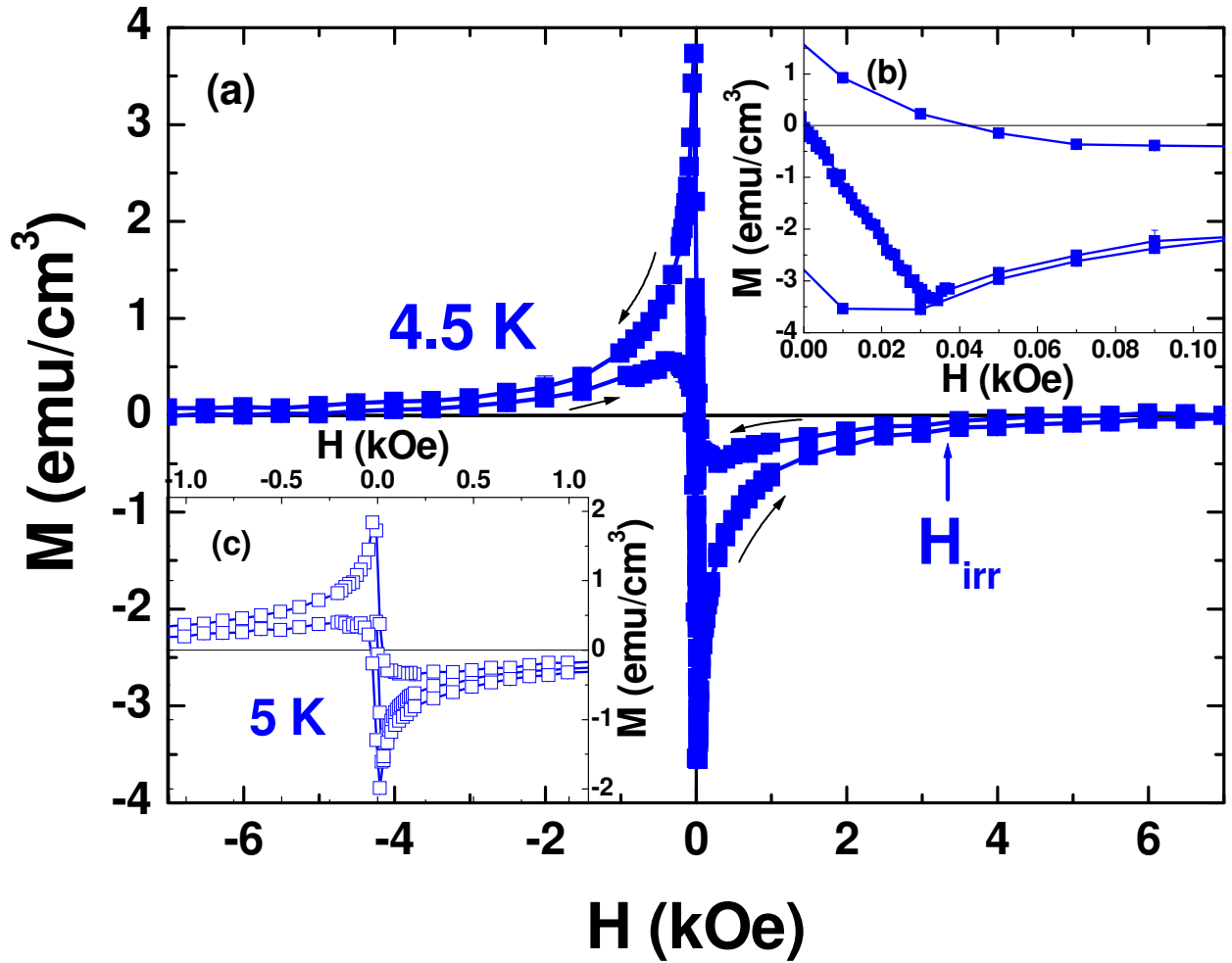


FIG. 3: Magnetization *vs.* magnetic field curves for RbOs_2O_6 single crystals. (a) Magnetization loop at 4.5 K . The irreversibility field determined from ZFC-FC $M(T)$ measurements is indicated. (b) Zoom of the magnetization in the low-field region allowing a detailed observation of the Meissner branch. (c) Magnetization loop of RbOs_2O_6 at 5 K .

ing fraction consistent with the one estimated from the Meissner slope. The temperature $T_{c2}(H)$ is determined from the onset of the superconducting behavior in the ZFC and FC branches, as indicated in Fig. 4. The temperature at which the vortex magnetic response becomes irreversible on cooling, $T_{\text{irr}}(H)$, is identified as the point at which both branches merge. We obtained this temperature by plotting the difference $M_{\text{FC}} - M_{\text{ZFC}}$, see Fig. 4. For each applied field, no difference in the values of T_{irr} was detected when measuring at sweep rates of 25 and 5 mK per minute. Therefore, within this measurement-timescale the

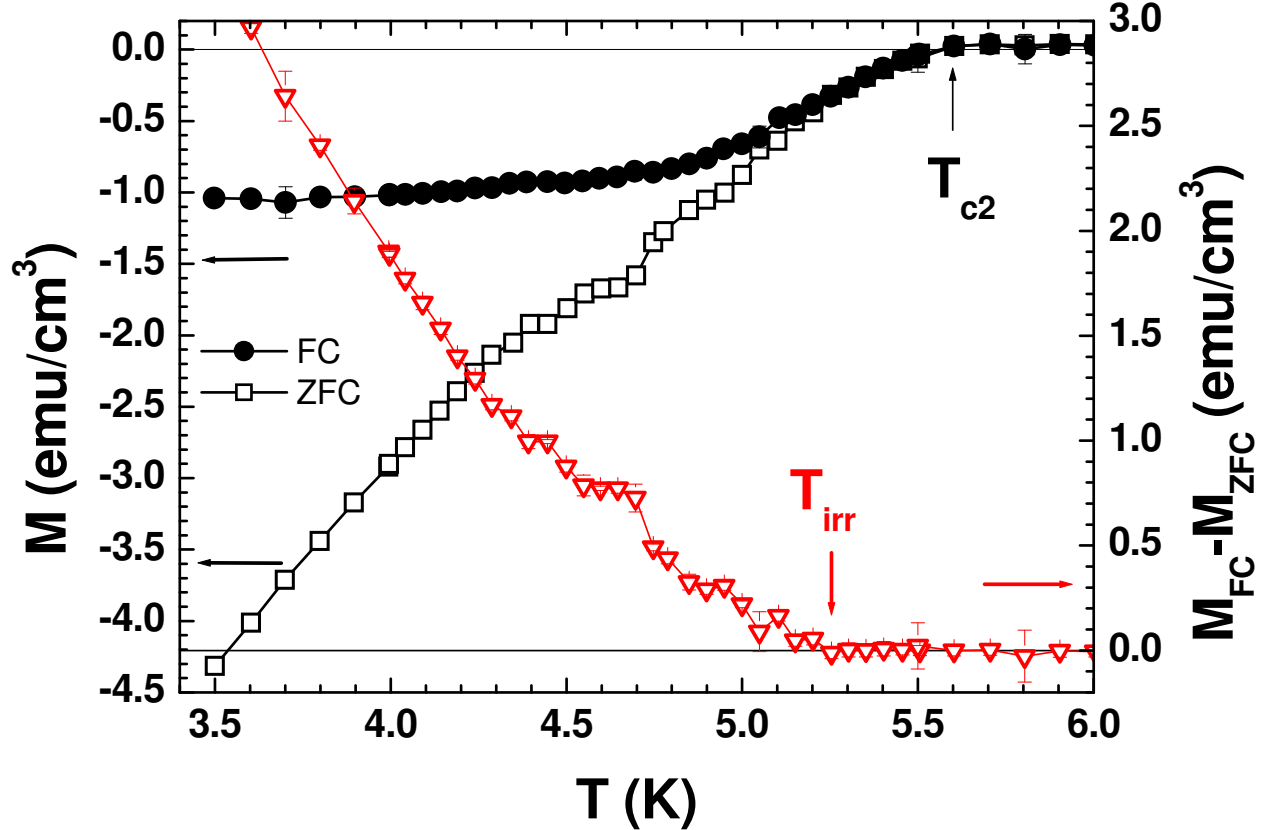


FIG. 4: Magnetization *vs.* temperature curves of RbOs_2O_6 following zero-field-cooling (ZFC) and field-cooling (FC) processes at an applied field of 100 Oe. The difference between both branches is considered in order to estimate the onset of the irreversible magnetic behavior at a temperature $T_{\text{irr}}(H)$. The upper critical temperature $T_{c2}(H)$ is estimated from the onset of screening.

obtained values of T_{irr} are not influenced by any dynamical effects.

Examples of ZFC-FC $M(T)$ curves at various applied fields are shown in Fig. 5. From the values of $T_{c2}(H)$ we obtained the upper critical field $H_{c2}(T)$ indicated in Fig. 7. In order to estimate the zero-temperature upper critical field, $H_{c2}(0)$, we fit $H_{c2}(T)$ with the Werthamer-Helfand-Hohenberg model (WHH) [21, 22, 23]. In the case of RbOs_2O_6 the Pauli paramagnetic critical field [24] $H_P \sim 18.4T_c = 101$ kOe is much larger than the $H_{c2}(0)$ obtained by linearly extrapolating $H_{c2}(T)$ down to zero temperature (~ 60 kOe), indicating a strong spin-orbit coupling. This last condition is fulfilled when $\alpha H/H_{c2}(0) \ll \lambda_{\text{so}}$, where λ_{so} is the spin-orbit scattering constant and α the Maki parameter [25]. In this limit, and in the absence of magnetic impurities, the Abrikosov-Gor'kov upper critical field equation reads (see Ref. [26] for an overview)

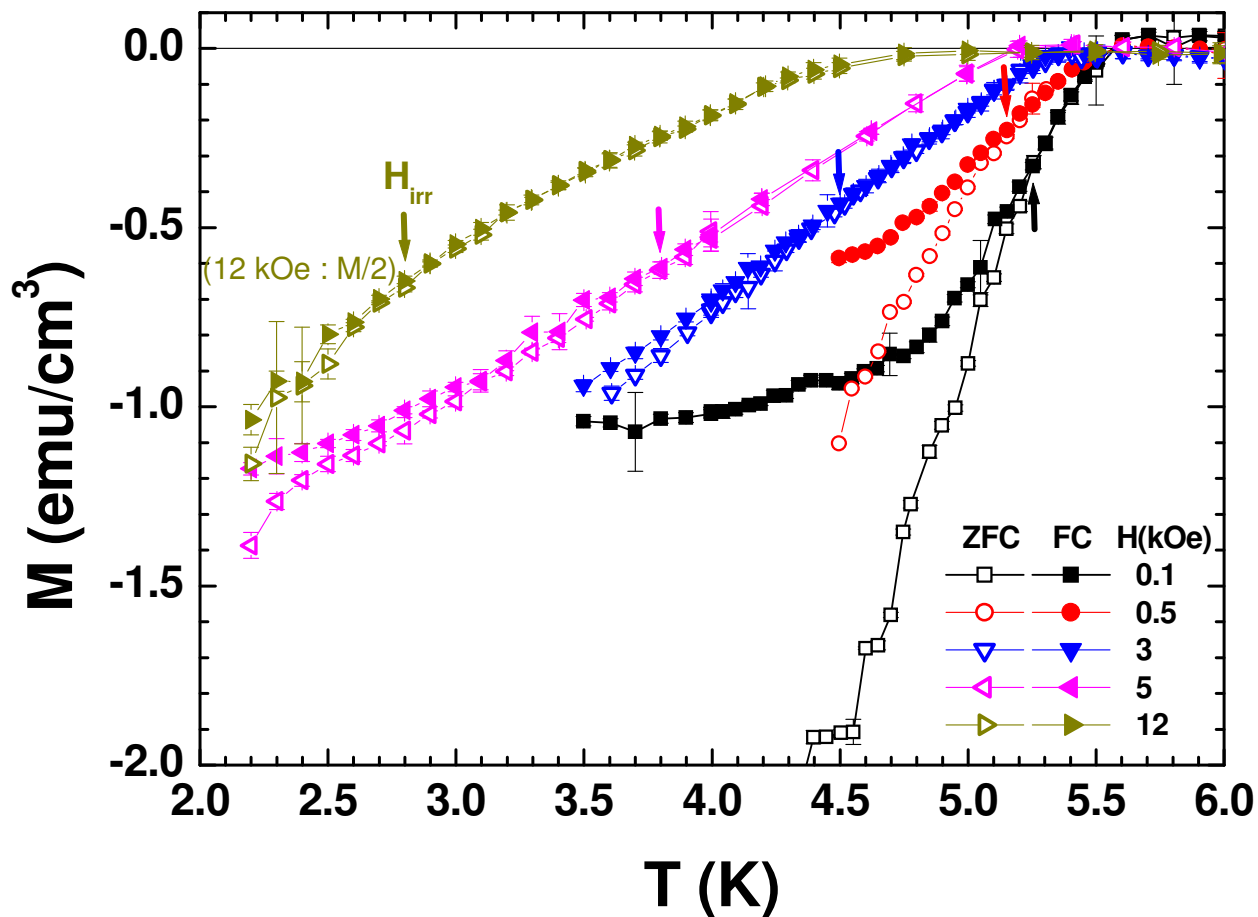


FIG. 5: Magnetization *vs.* temperature curves of RbOs₂O₆ following zero-field-cooling (open symbols) and field-cooling (full symbols) processes for various applied fields. The irreversibility temperature at each field $T_{irr}(H)$ is indicated with arrows. The measurements performed at 12 kOe are shown divided by a factor of two for clarity.

$$\ln\left(\frac{1}{t}\right) = \Psi\left(\frac{1}{2} + \frac{\rho_{AG}(t)}{2t}\right) - \Psi\left(\frac{1}{2}\right) \quad (1)$$

where Ψ is the digamma function, $t = T/T_c$, and $h_{c2}(t) = H_{c2}(t)/H_{c2}(0)$. The universal pair-breaking function

$$\rho_{AG}(t) = h_{c2}(t) + \frac{\alpha^2(h_{c2}(t))^2}{\lambda_{so}} \quad (2)$$

depends on λ_{so} and α . The latter is estimated from the slope of $H_{c2}(T)$ at the vicinity of T_c : $\alpha = -0.0528 \frac{dH_{c2}(T)}{dT}|_{T_c} = 0.75$ (H_{c2} in kOe) [23], whereas λ_{so} is a free parameter in the

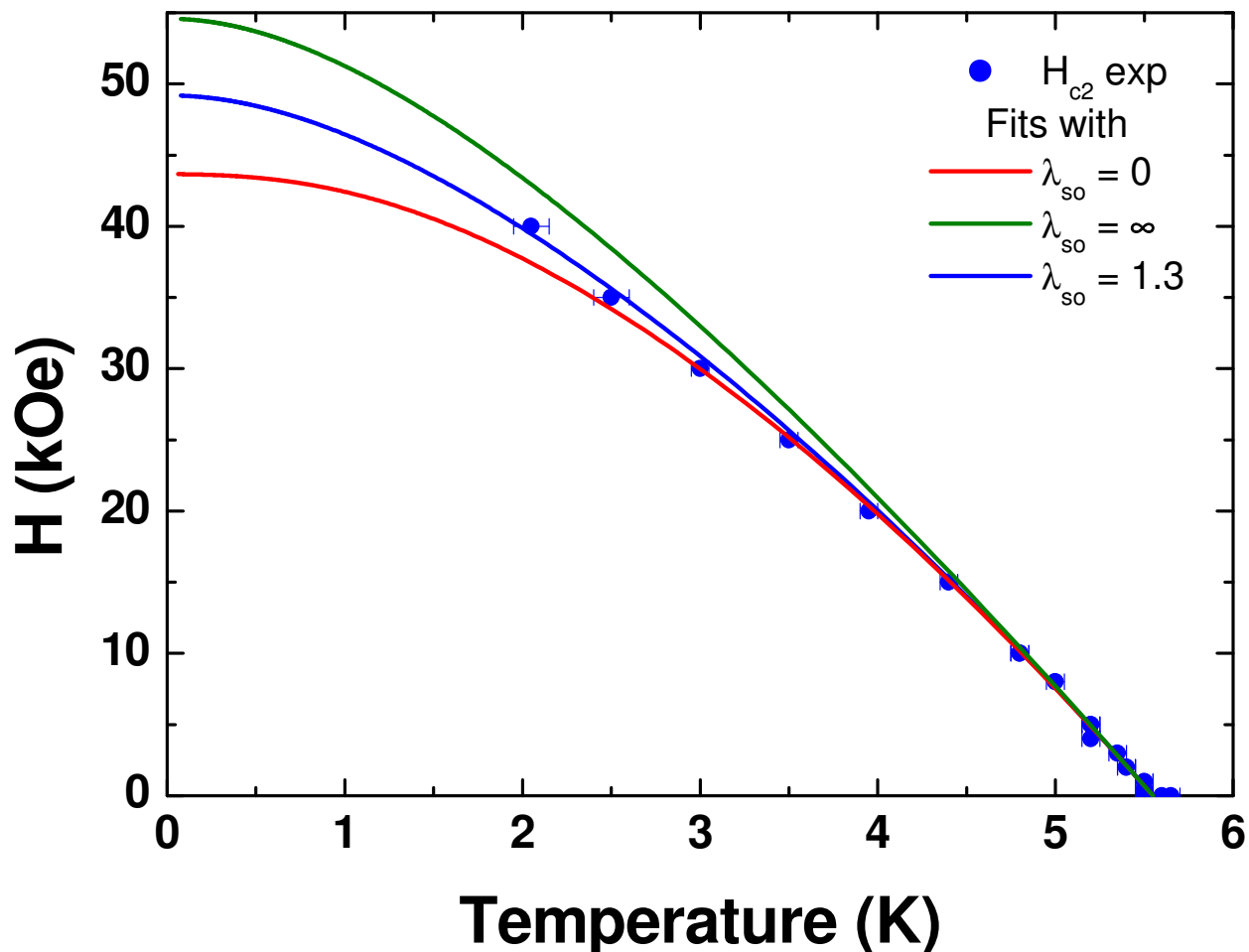


FIG. 6: Fits of $H_{c2}(T)$ with the WHH model [22, 23]. The experimental data is shown with blue symbols. The red line corresponds to the zero spin-orbit coupling case ($\lambda_{so} = 0$) whereas the green line is calculated using an infinite spin-orbit coupling ($\lambda_{so} = \infty$). The blue line is the best fit with a finite spin-orbit coupling of $\lambda_{so} = 1.3 \pm 0.2$.

fitting procedure. The best fit to the data with $\lambda_{so} = 1.3 \pm 0.2$ is presented in Fig. 6.

The same figure shows that considering a finite spin-orbit coupling is necessary to properly fit our experimental data. The curves obtained in the extreme cases of zero ($\lambda_{so} = 0$) and infinite ($\lambda_{so} = \infty$) spin-orbit coupling are shown with red and green lines. The latter curve was obtained using equations (1) and (2), whereas the former was obtained considering the general Abrikosov-Gor'kov equation in the $\lambda_{so} = 0$ limit [26]. It is evident that these two curves fail to properly fit the low-temperature data. The best fit to the data with $\lambda_{so} = 1.3 \pm 0.2$ therefore indicates that in RbOs_2O_6 the spin-orbit coupling can be considered

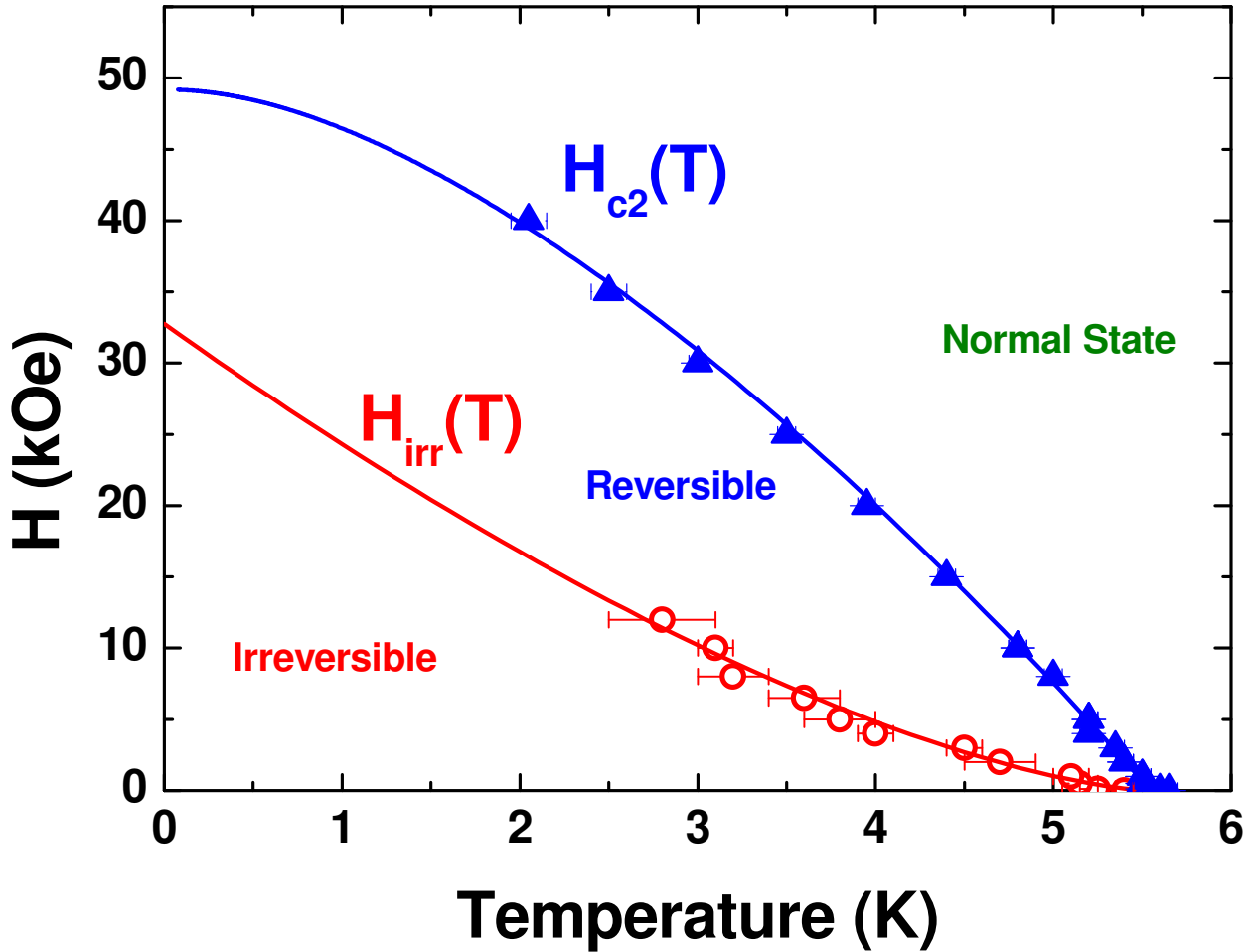


FIG. 7: Vortex phase diagram of RbOs_2O_6 : The upper critical field line, $H_{c2}(T)$, and the irreversibility line, $H_{irr}(T)$, are shown. The blue line is the best fit of the data using the WHH model [22, 23] which yields $H_{c2}(0) = 50$ kOe. The red line is a fit of H_{irr} with a temperature dependence proportional to $(1 - T/T_c)^{1.5}$.

to be moderately strong.

The fitted $H_{c2}(0) = 50$ kOe is roughly half H_P . Within the Abrikosov-Gor'kov theory we obtain a value of $H_{c2}(0)$ slightly smaller than that reported in Ref. [1] for other single-crystals. However, in that study the zero-temperature upper critical field was estimated from a fit of $H_{c2}(T)$ with an empirical power law [1]. Our fit within the Abrikosov-Gor'kov theory yields a coherence length $\xi(0) = \sqrt{\Phi_0/2\pi H_{c2}(0)} = 81$ Å. We therefore estimate a Ginzburg-Landau parameter $\kappa = 31$ by considering the penetration depth value obtained from muon-spin-rotation measurements in polycrystalline samples [27].

The vortex phase diagram of Fig. 7 also shows the locus of the irreversibility line, $H_{\text{irr}}(T)$, obtained from FC-ZFC magnetization *vs.* temperature curves. The most remarkable result shown in Fig. 7 is that the reversible magnetic response of RbOs_2O_6 spans an uncommonly wide region of the $H - T$ phase diagram. At low temperatures, $2.5 < T < 4 \text{ K}$, $H_{\text{irr}}(T)$ is of the order of $0.3H_{c2}(T)$. Figure 7 also shows that the irreversibility line can be well fitted with a sub-quadratic power law, $H_{\text{irr}} \propto (1 - T/T_c)^{1.5}$. These findings are in contrast with expectations for low- T_c superconductors. For example, NbSe_2 has a reversible region constrained to the vicinity of $H_{c2}(T)$ [28, 29, 30]. Furthermore, the irreversibility line in RbOs_2O_6 follows the same temperature dependence as those of typical high- T_c superconductors [31]. Although there is no systematic study of the temperature evolution of the irreversibility line in KOs_2O_6 crystals in the literature, one work reports that at 5 K ($t \sim 0.5$) the vortex response becomes reversible at fields higher than 10 kOe ($H_{\text{irr}} \sim 0.1H_{c2}$) [3]. Therefore, KOs_2O_6 seems to present an even wider reversible vortex region than RbOs_2O_6 .

An irreversible magnetic response in superconductors can have three different origins: bulk pinning, Bean-Livingston surface barriers [32] and geometrical barriers [33, 34]. In general, macroscopic magnetization measurements are not able to ascertain which of the three contributions is dominant when measuring an irreversible magnetic response that sets in at $H_{\text{irr}}(T)$. However, by conveniently modifying the sample geometry the effect of geometrical barriers can be affected. In the particular case of prism-like samples it has been shown that the effect of geometrical barriers in $H_{\text{irr}}(T)$ is negligible [35]. The Bean-Livingston surface barrier only produces a significant irreversible behavior in the case of extremely smooth surfaces [36]. In real samples with sharp corners and irregular edges, the effect of this barrier is of lesser importance. Therefore, as the crystals studied in this work are prism-like, $H_{\text{irr}}(T)$ can be considered as the field at which point pinning sets in while cooling, i.e. the depinning line. Strictly speaking, the effect of pinning may become relevant at slightly lower fields than $H_{\text{irr}}(T)$.

The depinning line is determined by the competition between thermal fluctuations and pinning generated by quenched disorder naturally present in the samples [37]. The magnitude of quenched disorder is typically measured by the dimensionless critical current-density ratio, $J_c(T, H)/J_0(T)$, with $J_0(T) = 4c\Phi_0/12\sqrt{3}\pi\lambda^2(T)\xi(T)$ the depairing current density [37]. For low- T_c superconductors this parameter is typically of the order of $10^{-2} - 10^{-1}$ whereas in high- T_c materials the pinning strength is weaker since $J_c/J_0 \sim 10^{-5} - 10^{-2}$

at low temperatures and fields. The relevance of thermal fluctuations increases with the Ginzburg number of the material, $G_i = 0.5(k_B T_c \gamma \kappa^2 / H_{c2}(0)^2 \xi(0)^3)^2$, proportional to the electronic anisotropy $\gamma = \sqrt{m_c / m_{ab}} \geq 1$ [37]. Typically, $G_i \sim 10^{-4} - 10^{-8}$ for low- T_c and $\sim 10 - 10^{-2}$ for high- T_c superconductors [37]. Therefore, both a small critical-current density ratio and a large Ginzburg number can conspire to produce a wide reversible vortex region.

The Ginzburg number $G_i = 6 \times 10^{-7}$ obtained for RbOs_2O_6 from the $H_{c2}(0)$ estimated in this work is within the range of values typically found for low- T_c materials. To obtain this value we assumed a negligible electronic anisotropy ($\gamma = 1$) based on the reported isotropic carrier mass for KOs_2O_6 [15] and the absence of similar data for RbOs_2O_6 . The value of G_i for RbOs_2O_6 indicates that thermal fluctuations are conventional and cannot account for the wide reversible vortex region. The Ginzburg number of KOs_2O_6 is one order of magnitude larger than that of RbOs_2O_6 . This is a consequence of $H_{c2}(0)$ ($\xi(0)$) being larger (smaller) in KOs_2O_6 (see Table II for numerical details). However, this larger G_i cannot account for the greater extent of the reversible vortex region in KOs_2O_6 : for example $H_{\text{irr}}(t = 0.5) / H_{c2}(t = 0.5) \sim 0.1$ and ~ 0.35 , for KOs_2O_6 and RbOs_2O_6 respectively.

For illustrative purposes, it is very interesting to compare the case of RbOs_2O_6 with that of NbSe_2 . Both compounds have similar T_c , λ and ξ , but NbSe_2 is more anisotropic with $\gamma = 3.3$, resulting in a Ginzburg number one order of magnitude larger than that of RbOs_2O_6 . However, the reversible vortex region in NbSe_2 is constrained to 0.1 K below $H_{c2}(T)$ [30] whereas in the case of RbOs_2O_6 it is much wider.

As a consequence, the wide reversible vortex region of RbOs_2O_6 has to be caused by a low critical current density. We estimated the critical current density, $J_c(T, H)$, assuming that the effect of surface and geometrical barriers is negligible. In this case, within the Bean model [42] the critical current density can be estimated from $M(H)$ loops as $J_c(T, H) \sim (c/f)\Delta M(T, H)$. Here $\Delta M(T, H)$ is the separation between the two branches of the magnetization loop at a field H , c the speed of light, and $f = (a/2)(1 - a/3b)$, where a and b are the dimensions in the plane perpendicular to the applied magnetic field. Figure 8 shows the $J_c(H)$ curves for temperatures of 4.5 and 5 K. As expected, the critical current density decreases with magnetic field and temperature and consistently becomes negligible at the irreversibility field determined from FC-ZFC magnetization measurements.

TABLE II: Measured and derived superconducting parameters for the β -pyrochlores RbOs₂O₆ and KOs₂O₆ and the low and high-T_c superconductors NbSe₂ and optimally-doped Bi₂Sr₂Ca₂Cu₃O₁₀.

Parameter	RbOs ₂ O ₆	KOs ₂ O ₆	NbSe ₂	Bi ₂ Sr ₂ Ca ₂ Cu ₃ O ₁₀
T_c [K]	5.5 ^a	9.6 ^d	7.2 ^{h,i}	110.5 ^k
$\xi(0)$ [Å]	81 ^a	31-37 ^d	77 ^h	$\sim 10^k$
$\lambda(0)$ [Å]	2500 ^b	2500-2700 ^{d,e}	2000 ⁱ	500 ^k
$\kappa = \frac{\lambda(0)}{\xi(0)}$	31	70-87	26	~ 50
γ	- ^c	$\sim 1^f$	3.3 ^h	27 ^k
$H_{c2}(0)$ [kOe]	50 ^a	340 ^d	55 ^h	~ 3000
$G_i = 0.5 \left(\frac{k_B T_c \gamma \kappa^2}{H_{c2}(0)^2 \xi(0)^3} \right)^2$	$5 \cdot 10^{-7}$ ^c	$5 \cdot 10^{-6}$	$5 \cdot 10^{-6}$	$2 \cdot 10^{-2}$
$J_c(t, h(T))/J_0(t)$	$5 \cdot 10^{-5}$ ^a	$5 \cdot 10^{-6}$ ^g	$3 \cdot 10^{-1}$ ^j	$1 \cdot 10^{-5}$ ^k
for $h(T) = 0.02$ and $t =$	0.81	0.52	0.59	0.16

^a This work, single crystals.

^b Ref. [27], polycrystals.

^c No data available in the literature. In order to calculate G_i we assumed $\gamma = 1$ (see text).

^d Ref. [12], single crystals.

^e Ref. [38], polycrystals.

^f Ref. [15], single crystals.

^g Critical current calculated by us from data of Ref. [3].

^h Ref. [39].

ⁱ Ref. [40].

^j Ref. [29].

^k Ref. [41].

According to the results in Fig. 8, for RbOs₂O₆ the critical-current density ratio $J_c/J_0 \sim 5 \times 10^{-5}$ for reduced temperature $t = 4.5/T_c = 0.81$ and field $h(T) = H/H_{c2}(T) = 0.02$. To estimate this ratio we have calculated $J_0(t)$ considering the two-fluid model expression for $\lambda(T)$ and $\xi(T)$ [37]. A similar critical current density ratio is obtained for a reduced temperature $t = 0.91$. These values of J_c/J_0 for RbOs₂O₆ are smaller than values typically measured for other low-T_c materials. For example, they are four orders of magnitude smaller

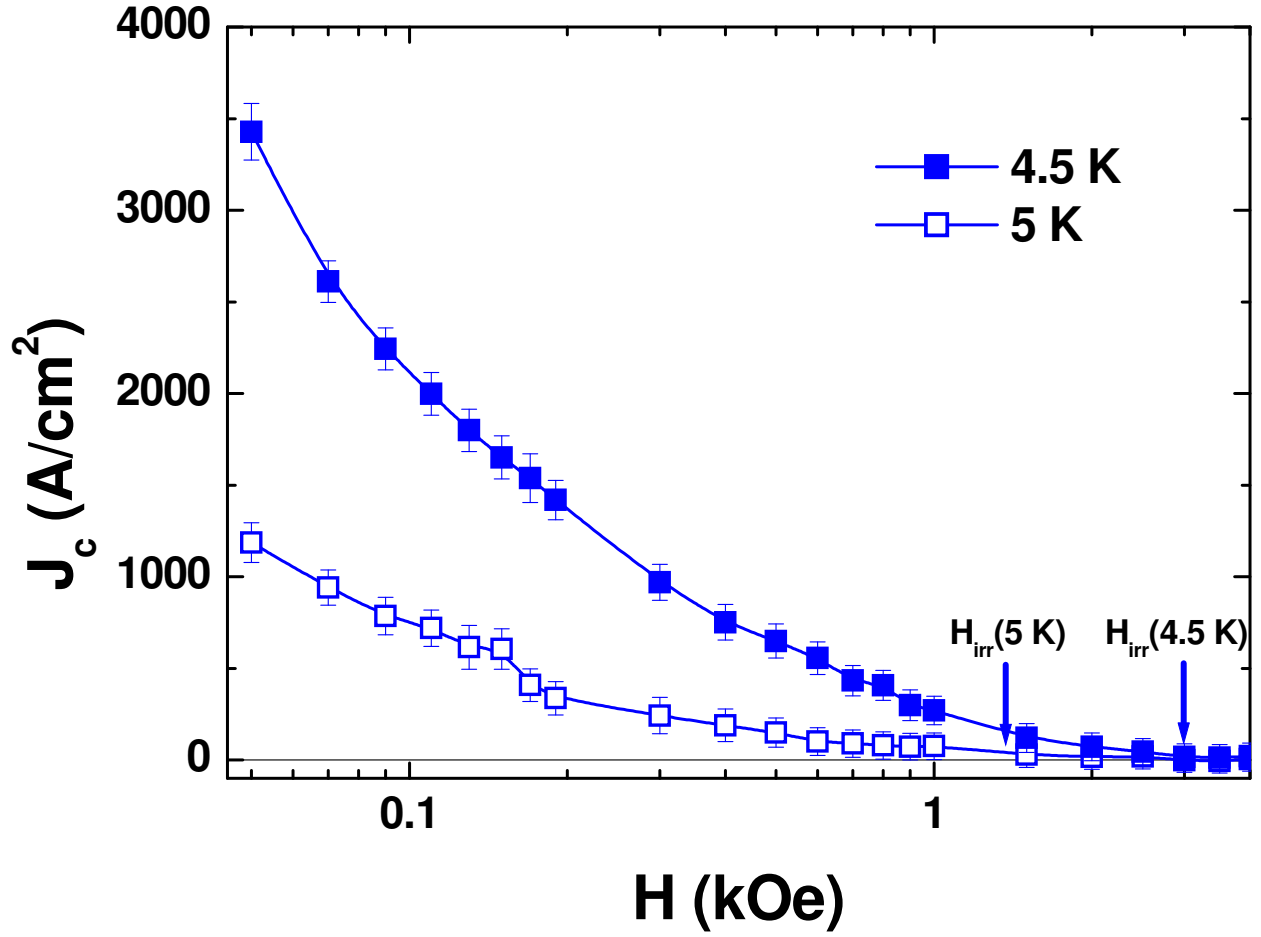


FIG. 8: Critical current density as a function of magnetic field for RbOs_2O_6 at 4.5 K (full squares) and 5 K (open squares). The irreversibility fields determined from FC-ZFC $M(T)$ measurements are indicated.

than that of NbSe_2 at the same reduced field [29]. Strikingly, the value of J_c/J_0 is comparable to that of high- T_c compounds: for example it is of a similar order of magnitude to that of $\text{Bi}_2\text{Sr}_2\text{Ca}_2\text{Cu}_3\text{O}_{10}$ at low fields and temperatures (see Table II). Therefore, in RbOs_2O_6 quenched disorder has an importance as small as in the case of high- T_c 's. In spite of T_c being much smaller, the low value of $J_c(T, H)/J_0(T)$ is at the root of the unusually wide reversible vortex region detected in RbOs_2O_6 .

A low magnitude of the critical-current density ratio might be generic to the β -pyrochlore family. In the case of KOs_2O_6 , although no data on $J_c(T, H)$ is available in the literature, we have considered the $M(H)$ data of Ref. [3] in order to estimate its critical current density

at 5 K and $h(T) = 0.02$. As shown in Table II, KOs_2O_6 has a $J_c(T, H)/J_0(T)$ one order of magnitude smaller than that of RbOs_2O_6 . The decreased relevance of quenched disorder would explain the suspected wider reversible vortex region of KOs_2O_6 [3].

CONCLUSIONS

In conclusion, we present the first data on the vortex matter phase diagram in RbOs_2O_6 single crystals [1]. We found that this compound presents a reversible vortex region that is unexpectedly wide for a low- T_c material. This finding might be generic to the β -pyrochlore osmate superconductors.

We found that this phenomenon originates from weak bulk pinning since the relevance of thermal fluctuations seems to be limited. The structural characterization results presented here suggest that the crystal defect density is very low in RbOs_2O_6 . This can explain the weak pinning magnitude. Surprisingly, the Rb and K members of the β -pyrochlore family present a critical-current density ratio comparable to that of high- T_c superconductors. Furthermore, resistivity measurements in KOs_2O_6 single crystals suggest an intrinsic pinning mechanism [8], a feature that is typically observed in high- T_c 's [43]. The evidence presented here therefore indicates that the negligible importance of bulk pinning produces a wide reversible region.

The authors acknowledge M. Decroux, F. de la Cruz, A. A. Petrović and G. Santi for useful discussions and A. Piriou and R. Lortz for assistance in the SQUID measurements. This work was supported by the MaNEP National Center of Competence in Research of the Swiss National Science Foundation.

-
- [1] K. Rogacki, G. Schuck, Z. Bukowski, N.D. Zhigadlo and J. Karpinski, Phys. Rev. B **77**, 134514 (2008).
 - [2] E. Yonezawa, Y. Muraoka, Y. Matsushita and Z. Hiroi, J. Phys.: Condens. Matter **16**, L9 (2004).
 - [3] G. Schuck, S. M. Kazakov, K. Rogacki, N. D. Zhigadlo, and J. Karpinski, Phys. Rev. B **73**, 144506 (2006).
 - [4] E. Yonezawa, Y. Muraoka, Y. Matsushita and T. Hiroi, J. Phys. Soc. Jpn. **73**, 819 (2004).

- [5] S.M. Kazakov, N.D. Zhigadlo, M. Brühwiler, B. Batlogg and J. Karpinski, *Supercond. Sci. Technol.* **17**, 1169 (2004).
- [6] M. Brühwiler, S.M. Kazakov, N.D. Zhigadlo, J. Karpinski and B. Batlogg, *Phys. Rev. B* **70**, 020503(R) (2004).
- [7] E. Yonezawa, Y. Muraoka, and T. Hiroi, *J. Phys. Soc. Jpn.* **73**, 1655 (2004).
- [8] Z. Hiroi, and S. Yonezawa, *J. Phys. Soc. Jpn.* **75**, 043701 (2006).
- [9] T. Shibauchi, M. Konczykowski, C. J. van der Beek, R. Okazaki, Y. Matsuda, J. Yamaura, Y. Nagao, and Z. Hiroi, *Phys. Rev. Lett.* **99** 257001 (2007).
- [10] C. Dubois, G. Santi, I. Cuttat, C. Berthod, N. Jenkins, A. P. Petrović, A. A. Manuel, Ø. Fischer, S.M. Kazakov, Z. Bukowski and J. Karpinski, *Phys. Rev. Lett.* **101** 057004 (2008).
- [11] Z. Hiroi, S. Yonezawa, J. I. Yamaura, T. Muramatsu, and Y. Muraoka, *J. Phys. Soc. Jpn.* **74**, 1682 (2005).
- [12] M. Brühwiler, S.M. Kazakov, J. Karpinski and B. Batlogg, *Phys. Rev. B* **73**, 094518 (2006).
- [13] R. Khasanov, D. G. Eshchenko, J. Karpinski, S. M. Kazakov, N. D. Zhigadlo, R. Brütsch, D. Gavillet, D. Di Castro, A. Shengelaya, F. La Mattina, A. Maisuradze, C. Baines and H. Keller, *Phys. Rev. Lett.* **93**, 157004 (2004).
- [14] T. Shibauchi, L. Krusin-Elbaum, Y. Kasahara, Y. Shimono, Y. Matsuda, R. D. McDonald, C. H. Mielke, S. Yonezawa, Z. Hiroi, M. Arai, T. Kita, G. Blatter, and M. Sigrist, *Phys. Rev. B* **74** 220506(R) (2006).
- [15] Z. Hiroi, S. Yonezawa, Y. Nagao, and J. Yamaura, *Phys. Rev. B* **76** 014523 (2007).
- [16] G. Sheldrick, SHELXL-97: Program for the Refinement of DCrystal Structures, University of Göttingen, Germany, (1997).
- [17] Oxford Diffraction Ltd. XCalibur, CrysAlis Software System, Version 1.170. (2003).
- [18] J. Yamaura, S. Yonezawa, Y. Muraoka, and Z. Hiroi, *J. Solid State Chem.* **179(1)** 336-340 (2006).
- [19] R. Galati, R. W. Hughes, C. S. Knee, P. F. Henry, and M. T. Weller, *J. Mater. Chem.* **17(2)** 160-163 (2007).
- [20] Z. Hiroi, S. Yonezawa, T. Muramatsu, J.-I. Yamaura, and Y. Muraoka, *J. Phys. Soc. Jpn.* **74**, 1255 (2005).
- [21] A. A. Abrikosov and L. P. Gorkov, *Soviet Phys. JETP* **12**, 346 (1961).
- [22] E. Helfand and N. R. Werthamer, *Phys. Rev.* **147**, 288 (1966).

- [23] N. R. Werthamer, E. Helfand and P. C. Hohenberg, Phys. Rev. **147**, 295 (1966).
- [24] A. M. Clogston, Phys. Rev. Lett. **9**, 266 (1962); B. S. Chandrasekhar, Appl. Phys. Lett. **1**, 7 (1962).
- [25] K. Maki, Physics **1**, 21, 127 (1964).
- [26] Ø. Fischer, Helv. Phys. Acta **45**, 329 (1972) and references therein.
- [27] R. Khasanov, D. G. Eshchenko, D. Di Castro, A. Shengelaya, F. La Mattina, A. Maisuradze, C. Baines, H. Luetkens, J. Karpinski, S. M. Kazakov, and H. Keller, Phys. Rev. B **72**, 104504 (2005).
- [28] W. Henderson, E. Y. Andrei, M. J. Higgins, and S. Bhattacharya, Phys. Rev. Lett. **77** 2077 (1996).
- [29] L. A. Angurel, F. Amin, M. Polichetti, J. Aarts, and P. H. Kes, Phys. Rev. B **56** 3425 (1997).
- [30] S. Mohan, J. Sinha, S. S. Banerjee and Y. Myasoedov, Phys. Rev. Lett. **98**, 027003 (2007).
- [31] M. Tinkham, *Introduction to Superconductivity* (Dover Publications, New York, 2004).
- [32] C. P. Bean and J. D. Livingston, Phys. Rev. Lett. **12** 14 (1964).
- [33] E. Zeldov et al., Phys. Rev. Lett. **73** 1428 (1994).
- [34] M. V. Indenbom, and E. H. Brandt, Phys. Rev. Lett. **73** 1731 (1994).
- [35] D. Majer, E. Zeldov and M. Konczykowski, Phys. Rev. Lett. **75** 1166 (1995).
- [36] P. G. de Gennes, *Superconductivity of Metals and Alloys* (Benjamin, New York, 1966).
- [37] G. Blatter, M. V. Feigel'man, V. B. Geshkenbein, A. I. Larkin, V. M. Vinokur, Rev. Mod. Phys. **66** 4 (1994).
- [38] A. Koda, W. Higemoto, K. Ohishi, S. R. Saha, R. Kadono, S. Yonezawa, Y. Muraoka, and Z. Hiroi, J. Phys. Soc. Jpn. **74**, 1678 (2005).
- [39] P. de Trey, S. Gyax and J. P. Jan, J. Low Temp. Phys. **11**, 421 (1973)
- [40] K. Takita and K. Masuda, J. Low Temp. Phys. **58**, 127 (1984) ; L. P. Le, Physica (Amsterdam) **185-189C**, 2715 (1991).
- [41] A. Piriou, Y. Fasano, E. Giannini, and Ø. Fischer, arXiv:0802.2617.
- [42] C. P. Bean, Rev. Mod. Phys. **36**, 31 (1964).
- [43] D. Feinberg, and C. Villard, Phys. Rev. Lett. **65** 919 (1990); R. A. Doyle, A. M. Campbell and R. E. Somekh, Phys. Rev. Lett. **71** 4241 (1993).